Aerosol Assisted Synthesis of Porous TiN_xO_y@C Nanocomposites

V. Maurice[a],*, G. Clavel[a], M. Antonietti[a], C. Giordano[a,b],*

Abstract: Porous TiN_xO_y based particles were synthesized by an aerosol spray process. At first, the starting sol solution containing the metal precursor and the nitrogen source is sprayed to form an aerosol that is subsequently pyrolysed at different temperatures. The obtained dried particles are an amorphous coordination "polymer" rich in carbon and nitrogen. These "glassy" particles are finally thermally treated at 800°C, promoting the crystallization of the particles and the release of a major part of the carbon. As the particles keep their original shape, carbon loss and density increase during the crystallization step and lead to the development of an accessible pore structure. The process was analyzed and was extended to the synthesis of other metal nitrides, such as VN and W_2N, thereby showing its general validity for the production of functional nanocrystalline nitride ceramics with high porosity still occupying a relatively small volume, and otherwise not easily accessible.

Introduction

Non-oxide ceramics, such as metal carbides and nitrides, have been used for a long time, mainly due to their hardness and good thermal resistance. Metal nitrides show -simplistically spoken- properties close to those of the corresponding metals, such as high electric conductivity and catalytic properties.[1] When combined with small sizes and high specific surface area, an extension of the current range of applications can be expected. Porous materials exhibit high specific surface area still occupying a relatively small volume and are thus ideal as supports for surface area driven applications, such as catalysis but also for chromatography, adsorption, separation, sensing, etc. In electrochemical applications, as well as in the fields of energy storage and photovoltaics, porous crystalline materials are a top choice, due to the combination of high surface area with good electrical transport properties.[2]

However, a strong limitation to be overcome in synthesis are the harsh synthetic conditions classically requested for the production of such ceramics, for instance temperature above 1000°C, long reaction times and use of strong nitrification agents (in case of nitrides). These extreme conditions usually promote growth to large particles, without any dimensional and morphological control on the final products.

[a] Dr. V. Maurice, Dr. G. Clavel, Prof. M. Antonietti, Dr. C. Giordano
Department of Colloid Chemistry
Max-Planck-Institute of Colloids and Interfaces
Research Campus Golm, D-14424 Potsdam, Germany
E-mail: cristina.giordano@mpikg.mpg.de
[b] New address: Stranski Laboratorium, Technische Universität Berlin
Straße des 17. Juni 124, D-10623 Berlin
cristina.giordano@campus.tu-berlin.de

Supporting information for this article is given via a link at the end of the document.

For the synthesis of metal nitrides and carbides under milder conditions, several sol-gel based routes have been applied,[2, 3] and among them, the so-called *urea-glass route (UGR)* was shown by our group to be a simple and fairly sustainable way to produce several nitrides and carbides under rather mild conditions, using non-toxic reagents and avoiding the use of corrosive ammonia.[4]

In the present paper the UGR is coupled to an aerosol technique, which uses the flexible sol-gel nature of the intermediates to introduce additional structural parameters.

Aerosol techniques have been extensively used to produce porous and non-porous oxide particles,[5] but only a few studies have focused on the production of non-oxide ceramics. For the generation of nitrides, the process usually involves two steps: first, the synthesis of the intermediate particles (generally an oxide or oxynitride phase) by pyrolysis of a precursor solution, and then a subsequent nitridation of the obtained products to crystallize the desired material.[6, 7] To our knowledge, only one study has described the synthesis of porous titanium nitride particles using aerosol spray, taking advantage of the formation of an intermediate porous zinc titanate phase, in which the zinc serves as template during the subsequent reduction with ammonia at 1000°C. Due to recrystallization during the reduction, the surface area of the particles is still rather low (17 m²/g).[8]

In the present work, we coupled the urea-glass route with aerosol spraying, purposely tailored for the production of porous metal nitrides at moderate temperature (800°C) without the need for ammonia or any additional templating agent. The synthetic strategy consists of: first a tailored precursor complex made of a metal salt and a nitrogen source is prepared. In these specific precursors, the nitrogen source should be a multidentate ligand (such as urea or dicyanoimidazole), so the metal and the nitrogen source can form a glassy, disordered coordination polymer, pre-organizing the reactants. Secondly, the precursor solution is sprayed, dried and partly pyrolyzed towards solid intermediate particles. In the final step, the produced material is thermally treated under N_2 flow to allow the crystallization of the desired phase. The composition of the precursor solution is a key parameter to obtain a nitrogen rich intermediate glass, which does not require the use of further nitridification agents to convert to the oxynitride phase.

Within the aerosol generator, particle shape and size can be controlled. It will be shown that the drying temperature influences the properties of the produced particles, notably the advancement of the organic precursor decomposition, which indirectly allows controlling the porosity of the produced particles. Control of the oxygen content is the critical point to avoid oxidation of the metal. The process has been studied to determine the conditions that allow the synthesis of the nitrides with the lowest oxygen content. The produced materials were analyzed by XRD, TEM, Elemental Analysis, Infrared spectroscopy and N_2 adsorption.

TiN_xO_y synthesis has been used as a proof of concept in this contribution, but vanadium nitride and tungsten nitride were also

made using the same procedure. Therefore, this process can be considered as a general way of producing metal nitride particles with a secondary porous bead structure by aerosol synthesis.

Results and Discussion

A schematic representation of the synthetic process is reported in figure 1. The two heating steps will be named pyrolysis step and second heating step respectively. The term second heat treatment will be used to indicate the final heat treament performed under N_2 flow, during which the TiO_xN_y phase crystallizes.

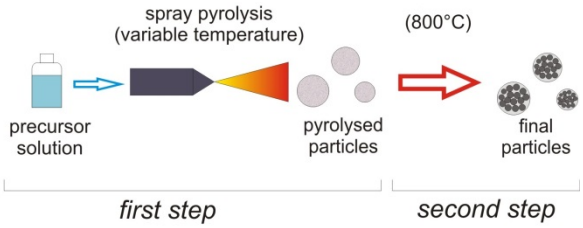

Figure 1. Scheme of the synthesis process.

1. Spray pyrolysis

In this first step the metal precursor complexes, prepared using DI and urea as nitrogen source, are sprayed and pyrolized at different temperatures (namely 400, 600 and 800°C). In each case a solid powder is obtained, which was analyzed by XRD to get information about crystallinity and structure of the products. Figure 2 reports the patterns of the samples prepared using DI (panel A), urea (panel B) and both DI+urea together (panel C).

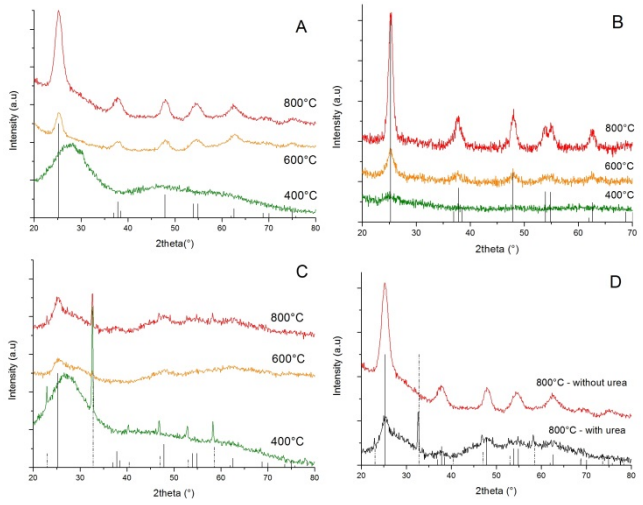

Figure 2. XRD patterns of the particles after the pyrolysis step at various temperatures: A) using only DI; B) using urea only; C) using both DI and urea. D) comparison of the patterns obtained with and without urea at 800°C. The reference patterns of anatase (ICDD 01-075-2545, vertical lines) and NH_4Cl (ICDD 01-089-2786, dashed vertical lines) are also reported for comparison.

In panel D, the diffractograms of samples pyrolized at 800 °C with and without the assistance of urea to DI are reported for a closer comparison. From this figure, the strong influence of the temperature on the crystallinity of the particles, as well as the influence of the nitrogen source used, can be clearly seen. For lower temperatures (400-600°C), in each case mainly an amorphous phase is observed. Upon further increase of the temperature (up to 800°C), an anatase phase (namely TiO_2) is observed in the samples prepared using DI and urea separately, which is more defined (crystalline) in case of urea.
However, for the samples prepared using both precursors together (DI+urea), the majority of the samples is still amorphous even at higher temperature, probably in a sort of condensed precursor glass. The combined action of DI and urea is capable of avoiding the formation of anatase during the first step. The apparent low quality of the patterns is due to the fact that the materials are mostly amorphous. In no case a TiN phase is observed at this step, probably because the residence time in the heated zone of the aerosol set-up is too short to allow the crystallization. For instance, in previously reported syntheses,[4,9] the samples were treated at 800°C up to 12 hours. A way of improving the crystallization rate during pyrolysis would be to increase the oven temperature, but the condensation of acetonitrile takes place at a tube temperature of 850-900°C and creates a polymeric oily liquid that blocks the filter very quickly. Circumventing this problem could probably allow synthesizing the nitride phase directly during the pyrolysis step. Here, it is worth to mention that the use of ethanol (typical solvent of the urea-glass route) had to be avoided since it provides too much oxygen and hinders the formation of TiN (well crystallized titanium oxide was obtained in each case). Therefore acetonitrile has been used as an oxygen-free solvent.

Finally, in order to have an ideal starting solution, the metal concentration has been set under 3%, to keep a low viscosity and ease the spraying process.
The elemental analysis, performed on the samples obtained after pyrolysis (first heat treatment) and after calcination (second heat treatment) are reported in Table 1 and Table 2 respectively. Table 1 shows that, after the first heat treatment, the amounts of carbon, oxygen and nitrogen are comparable in this condensed precursor glass, independently from the temperature. However, the nitrogen and carbon contents are much higher than in the samples made using DI or urea separately (see supporting information S1). DI is a good carbon source and helps reducing oxidation, while urea acts as a nitrogen source. The presence of chlorine was observed by EDX spectra (see supporting information S2). The Cl amount (originating from the $TiCl_4$ precursor) is decreasing with increasing temperature, as expected for this rather volatile element.

Table 1. Elemental analysis performed on samples pyrolyzed at different temperatures.

Pyrolyzed samples	N %w/w	C %w/w	O %w/w	H %w/w	Ti %w/w
TiD0.5U1-400	17	15	nm	2	18
TiD0.5U1-600	18	17	18	1	37
TiD0.5U1-800	20	21	25	1	33

Table 2. Elemental analysis performed on samples after calcination step at 800°C.

Calcined samples	N %w/w	C %1/w	O %w/w	H %w/w	Ti %w/w
TiD0.5U1-400-R	12	15	13	1	50
TiD0.5U1-600-R	12	11	13	1	54
TiD0.5U1-800-R	11	13	12	1	44

The samples are named as follows: TiDxUy-T(-R), see Table 1
-Dx meaning the number of equivalents of DI
-Uy being the number of urea equivalents
-T being the temperature of the final aerosol drying.
-The suffix –R (from the French "*recuit*" and the Italian "*ricotto*") indicates the "re-cooked" samples, i.e samples heat treated a second time after the pyrolysis step. The second treatment occurs in oven at 800°C under N_2 flow.

The combination of urea and DI was also found to be crucial to reduce oxide formation and increase the nitrogen content. The addition of urea allows increasing the nitrogen content in the pyrolysed product and also decreases the oxidation risk compared to the samples produced with only DI (as clearly seen on the samples pyrolysed at 800°C, figure 2 panel D). On the figure S3, it is also clear that the main IR band is due to titanium oxide (sharp peak under 900 cm^{-1}).This is in all probability due to the NH_3 releases during the decomposition of urea,[10] which works as stronger *in-situ* nitrification agent. The reaction between ammonia (from the decomposition of urea) and hydrogen chloride (from the decomposition of $TiCl_4$) during the pyrolysis step is responsible for the formation of NH_4Cl observed on the XRD patterns. This phase (NH_4Cl) however disappears after the second heat treatment. From table 1 can be also seen that the titanium percentage is below 40%, somehow indicating that a significant part of the particles obtained after pyrolysis consists of an organic matrix, which decomposes upon further heat treatment, bringing porosity to the final material.

The intermediate products obtained after aerosol pyrolysis were also analyzed by infrared spectroscopy to determine the nature of the organic species present after this first step (figure 3).
With increasing temperature, the particles undergo a transition from the dried organometallic glass to a mixed amorphous carbon rich phase, best seen at 800°C. No pure chemical compounds are formed during this step, as these particles are only a reactional intermediate formed after a very short thermal treatment. During the pyrolysis step, the organic and inorganic compounds present in the precursor solution are decomposed by heat. Depending on the pyrolysis temperature, different chemical bonds can be observed by IR-spectroscopy, helping to understand the process.
At 400°C tube temperature, the gel is apparently simply dried and even keeps its yellow color (figure 3). The sample contains C-H and N-H bonds visible in the 3300-2900 cm^{-1} area, along with the CN peak at 2237 cm^{-1}, characteristic of the DI. The peak at 2193 cm^{-1} next to the cyanide is either due to the interactions of the metal with the cyanide groups of the DI, which lowers their vibration frequency, or it can also be attributed to the presence of urea condensation products (e.g. cyanuric acid).[10] The signal of the urea is broadened and shifted, due to metal interactions and/or condensation, but some corresponding peaks are visible in the 1700-1250 cm^{-1} zone.

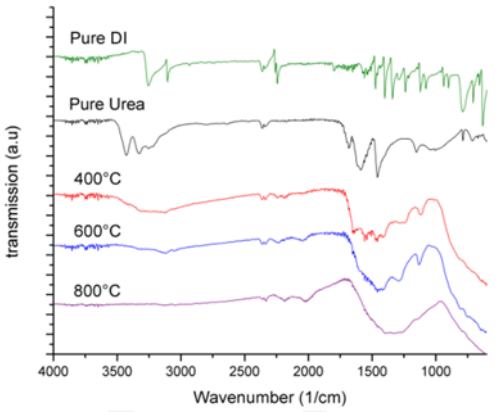

Figure 3. IR spectra of particles sprayed at different temperatures, using the ratio TiD0.5U1.

The appearance of the band at 1120 cm^{-1}, could be due to C-N aliphatic bonds probably present in the nitrogen rich carbon matrix that starts to form.[11] At 600°C tube temperature, the decomposition of the gel continues further, along with formation of the nitrogen rich carbon network. The particles have now a brown color. The observed bands are more broadened than at 400°C; the hydrogenated part of the spectrum (around 3500-3000 cm^{-1}) has a decreased intensity, indicating the further decomposition of urea and DI. The cyanide band is still present on the spectrum, and is broadened. A broad band at about 1500 cm^{-1} is now observed; this feature is typical for nitrogen doped amorphous carbon materials, it is caused by the presence of C=C and C=N bonds.[11, 13] The band centered at 1280 cm^{-1} can be attributed to the aliphatic C-C bonds forming a part of the network, which hosts the Ti ions. The elemental analysis further proves that the sample contains 17% and 18 % of carbon and nitrogen respectively. The hydrogen content has decreased to 1.5%, which is about half the value than for the 400°C sample.
At 800°C, the particles are black and the degradation of the organic precursors has advanced further. In the IR spectrum, one broad feature is observed between 1600 and 1000 cm^{-1}, which is once again characteristic of nitrogen-doped amorphous carbon.[11, 13]. The particles are still amorphous, possibly because the residence time in the heated zone is too short. They consist of an amorphous Ti(C,N) material (as observed by XRD). In summary, IR spectroscopy after pyrolysis at different temperatures shows the progressive decomposition of the urea and DI to form an amorphous carbon network doped with nitrogen, in which the Ti ions are dispersed. The particles are mostly amorphous, as shown by XRD.
In order to have information about size and morphology of the final particles, TEM investigation has been performed and images are reported in Figure 4. At any temperature, spherical particles are obtained, they show a diameter around 100 nm and a relatively large polydispersity index of 1.5 (calculated with the size distribution of 150 particles from TEM pictures). However, while at lower pyrolysis temperature the particles are entirely amorphous (see supporting information S4), at 800°C a few crystallites (lattice fringes) can be seen in high resolution pictures (see supporting information S5). The interplanar distances (around 0.34 nm) were tentatively ascribed to anatase or nitrogen doped titanium oxide.

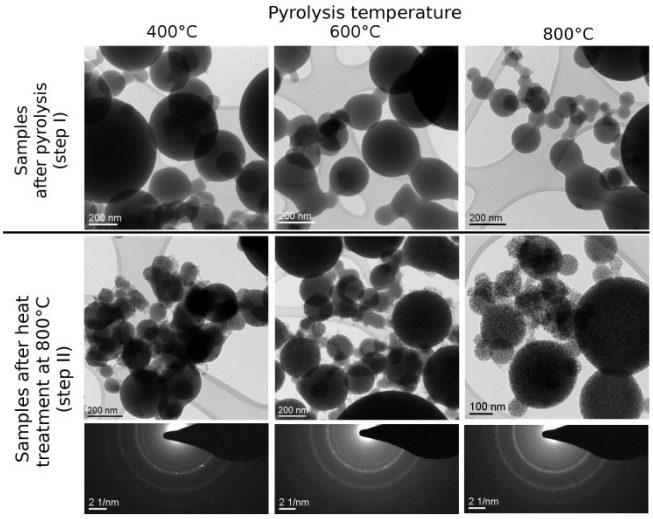

Figure 4. Particles dried at 400, 600 and 800°C respectively from left to right, before (upper row) and after the second heat treatment with corresponding SAED (bottom rows).

2. Second heating Step under N_2 flow

In this second (and last) step, the particles collected after aerosol pyrolysis (prepared using both DI and urea), were further heat-treated in an oven under nitrogen flow at 800°C for 3h to allow the crystallization of the desired phase. XRD patterns obtained after calcination are reported in figure 5.

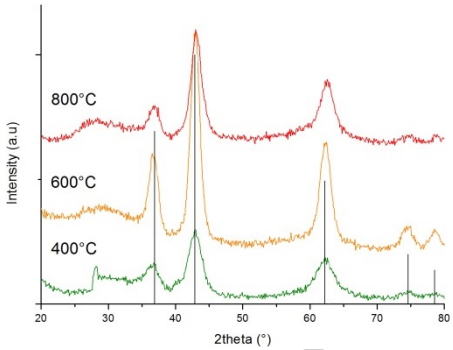

Figure 5. XRD patterns of the particles made 0.5 eq of DI and 1 eq of urea dried at different temperatures and subsequently heat-treated at 800°C for 3h (reference pattern: TiN, ICDD 00-038-1420).

In every case, the only crystalline phase observed has a cubic structure and shows a pattern slightly shifted compared to the one of pure TiN. Even if a poorly crystallized anatase phase was present after pyrolysis, during the final thermal treatment it is completely converted into the TiN_xO_y phase. It can also be noted that the intermediate products made using only urea turn to anatase after the second heat treatment, no TiN is observed (see figure S6). The amorphous carbon/nitrogen matrix can indeed serve as source of nitrogen and reduce the titanium oxide to nitride, as shown by Jun *et al.*[3] The thermal treatment was set at 800°C, as it is the lowest temperature allowing the crystallisation of the TiN_xO_y phase. From the XRD spectra, the average size of the crystallites was calculated by the Scherrer's formula (Table 3). The crystal size, close to 6 nm in each case, is not really influenced by the pyrolysis temperature.

Table 3. BET measurements and Scherrer size estimation results for the calcined particles.

Pyrolysis temperature (°C)	**400**	**600**	**800**
Average crystal size by TEM (nm)	4.8	6.2	5.8
Average crystal size by Scherrer equation (nm)	5.6	6.1	5.8
Surface area after calcination at 800°C (m^2/g)	79	164	187
Pore Volume after calcination at 800°C (cc/g)	$9.5 \cdot 10^{-2}$	$1.3 \cdot 10^{-1}$	$1.7 \cdot 10^{-1}$

The TEM pictures, made on the samples after calcination, show that the particles have an internal structure (Figure 4 bottom row and supporting information S7). They consist of many small nanoparticles inter-grown embedded in an amorphous matrix, which constitute the secondary aerosol particles. The average size of the primary particles observed by TEM is in agreement with the values obtained with XRD. SAED measurements on one or few secondary aerosol particles as well as the power spectrum of high resolution TEM (supporting information S7) confirm their polycrystalline nature and indicate a random orientation of the primary particles. From the N and Ti composition of the samples (Table 2), it can be seen that the Ti/N ratios are slightly higher than what is expected for a TiN composition. Furthermore, the diffraction peaks are shifted towards higher angles. The presence of carbon in the crystalline structure can be ruled out as the peaks expected for TiC are shifted to lower angles than TiN peaks. It can then be assumed that the Ti atoms in excess are bound to O atoms and from there, the level of oxygen bound to Ti can be estimated. For all the samples, a contamination of less than 5 wt% of O bound to Ti was calculated. The rest of the oxygen is probably molecularly dissolved into the carbon forming the matrix that holds the particles together.

The TiN_xO_y composition of the material was also supported by electron energy loss spectroscopy (EELS) (see supporting information S8). EELS spectra were recorded in the energy range covering the carbon, nitrogen and oxygen K edges as well as the titanium $L_{3,2}$ edges and, at regions containing different distributions of particles in order to draw conclusions about composition homogeneity. A comparison of the recorded spectra of the samples after the calcination step and a reference sample of TiN shows that the energetic position of the Ti L_3 and L_2 "white lines" as well as the structure of the nitrogen K edge matches well with the one of TiN. Moreover, for all the samples, a oxygen K edge having a similar shape that the one of N is always observed, suggesting a same local environment for oxygen. Although the integrated intensities of the different edges are a sensible measure for their relative quantity, in the present case, due to the proximity of the Ti, N and O edges, the background subtraction cannot be performed precisely preventing a determination of those quantities. Nevertheless, based on the overall similarity between the spectra, a homogeneous distribution of oxygen in the titanium nitride particles can be concluded. Furthermore, EELS experiments confirm that amorphous carbon is present all over the primary particles.

The elemental analysis performed on the samples after calcination shows a drastic reduction of the nitrogen and carbon percentage (table 2), almost 50% relative loss. This loss is what creates the pores, i.e. porosity is created by mass loss due to chemical reduction and the density increase throughout crystallization, leaving an interstitial void system between these small particles (see figure 6). The specific surface area of the particles has been measured; the results are reported in table 3 (and supporting information S9). All the samples show a surface area value over 70 m²/g, confirming the porosity of the nanocomposite. Indeed, non-porous spheres of the same size would have a surface area of 11 m²/g. Interestingly, there is a strong influence of the temperature applied during the first step on the specific surface area: it increases with the pyrolysis temperature. This effect can be attributed to the chemical nature of the particles obtained at the end of the aerosol pyrolysis step. As stated in the previous paragraph, at low pyrolysis temperatures, the particles have a strong organic character. Upon calcination, the slow heating rate in the nitrogen oven allows rearrangements of the structure and thus pore collapse and sintering. On the contrary, for the samples pyrolyzed at higher temperatures, the amorphous carbon network is well formed and rather rigid, i.e. they have a strong inorganic character. During the calcination, few rearrangements of the structure are possible because the carbon network firmly holds the structure together. Therefore the porous structure is kept when the matrix reacts.

The pore size distributions estimated by nitrogen absorption technique are similar at the different temperatures used in the pyrolysis step, with the pores being usually distributed between 3 and 8 nm, which is typical for the interstitial pores of TiN nanoparticles with the described size (see also supporting information S9).

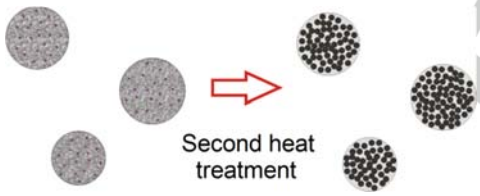

Figure 6. Scheme of the conversion of the particles obtained from step 1 to porous TiN_xO_y nanocomposites obtained after the second heat treatment.

3. Tests with other metals

Vanadium oxytrichloride and tungsten(IV) chloride have been sprayed under the same conditions as for the titanium precursor, in order to determine if this method could be applied to different metal systems. The samples were produced using 0.5 eq of DI and 1 eq of urea. Spraying and pre-pyrolysis was done at 600 °C tube temperature, calcination at 800°C, following the process described in the previous paragraphs. The XRD showed that in both cases the nitrides of the respective metals are obtained (figure 7). The peaks of the tungsten nitride are very broad and slightly shifted, which could be attributed either to very small crystallites or to the presence of carbon impurities.

This shows that this method is in fact efficient to produce different metal oxynitrides or nitrides.

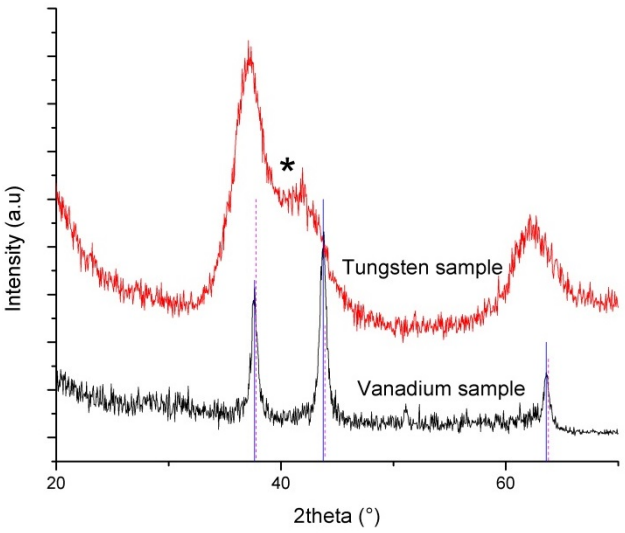

Figure 7. XRD patterns of vanadium nitride and tungsten nitride produced by aerosol synthesis (reference patterns: VN (continuous line), ICDD 00-035-0768; W_2N (dotted line), ICDD 00-025-1257; marked peak was tentatively attributed to W_2C, ICDD 04-014-5679).

Conclusions

Porous metallic ceramic particles have been synthetized by coupling an aerosol spray process with the urea-glass route. Exemplarily, porous TiN_xO_y nanocomposites (primary crystal size of ~6 nm) have been produced, and synthetic details were discussed. The formation of a suitable starting complex was shown to be fundamental to get a sufficient nitrogen amount in the intermediate particles and to minimize the residual amount of oxygen after the pyrolysis step. These particles have been subsequently turned into the porous TiNxOy@C nanocomposites without using any templating or nitriding agent. The pyrolysis temperature has a strong influence on the porosity and surface area of the final materials. Furthermore, the process was shown to be general and allow the production of other key metallic ceramic such as VN and W_2N. The presented process thus allows an easy manipulation of materials otherwise not easily processable, permitting for instance the deposition of the aerosol particles on a substrate directly after the first step, thus producing porous metal nitride layers, which would be very suitable for further applications, such as catalysis or energy storage due to the combination of high surface area with good transport properties.

Experimental Section

Spraying experiments

The precursor solution was made by dissolving 1g (5.2 mmol, 1eq) of $TiCl_4$ in 50 mL of dry acetonitrile (ACN). A clear yellow solution is obtained, to which 300 mg (2.5 mmol, 0.5 eq) of 4,5-dicyanoimidazole (DI) as a multidentate ligand were added. After DI is dissolved, 300 mg (5 mmol, 1eq) of urea were added, too. The solutions are stirred until complete dissolution of the solids.

The solution was then sprayed using a TSI 3076 nebulizer. The spraying gas was Argon at a flow rate of 2 L/min. The aerosol flow is carried

through a 1 m long tube of 100 mm diameter, where the droplets are pre-dried by natural evaporation. Finally the particles enter a quartz tube furnace heated to various temperatures; the heated length is 300 mm and the diameter is 60 mm. The residence time in the heated zone is about 15 s. After the spray pyrolysis, the particles are collected on a filter and heat treated in an oven under nitrogen at 800°C for 3h.

Experiments using separately 4,5-dicyanoimidazole and urea as nitrogen sources have been performed, as well as using both molecules together. The combination of DI and urea was found to be ideal to decrease the oxidation risk during synthesis and increase crystallinity of the final TiN_xO_y. In Table 1 and 2 the results of the elemental analysis performed on samples pyrolyzed at different temperatures and after calcination step at 800°C are reported.

Analyses

The products were analyzed by XRD, elemental analysis, HRTEM and BET. Species identification was performed according to elemental analysis and X-rays diffraction (by ICDD-PDF4+ database). XRD measurements were performed on a D8 Diffractometer from Bruker instruments (Cu K□ radiation, λ = 0.154 nm) equipped with a scintillation counter. Nitrogen sorption experiments were done with a Quantachrome Autosorb-1 or Quadrasorb at liquid nitrogen temperature, and data analysis were performed by Quantachrome software. All the samples were degassed at 150°C for 20 h before measurements. Elemental analysis was done for Carbon, Hydrogen, Nitrogen and Oxygen using a Vario EL Elementar. ICP OES analysis was carried out using an ICP OES Optima 2100 DV (Perkin Elmer). TEM images were taken using a Zeiss EM 912Ω operated at an acceleration voltage of 120 kV. Samples were ground and then suspended in ethanol. One drop of this suspension was deposited on a 400 mesh carbon-coated copper grid and left in air to dry. High resolution microscopy, EELS and EDX measurements were performed on a Philips CM 200 FEG microscope operated at an acceleration voltage of 200 kV and equipped with a post column EELS spectrometer (GATAN Tridiem). IR spectra were recorded in the ATR geometry using a Varian FTS 1000 between 650 and 4000 cm^{-1}.

Acknowledgements

The authors wish to thank the Max Planck Society for financial support and the Fritz Haber Institute of the Max Planck Society for high resolution TEM.

Keywords: Metal nitride • Urea glass route • Aerosol spray • Porous • Nanoparticles

[1] W. Lengauer, in *Handbook of Ceramic Hard Materials*, ed. R. Riedel, WILEY-VCH Verlag GmbH, Weinheim, 2000, ch. 7, p. 202

[2] (a) P. Han, Y. Yue, X. Wang, W. Ma, S. Dong, K. Zhang, C. Zhang, G. Cui, *J. Mater. Chem.*, **2012**, *22*, 24918; (b) E. Ramasamy, C. Jo, A. Anthonysamy, I. Jeong, J. K. Kim, J. Lee, *Chem. Mater.* **2012**, *24*, 1575−1582; (c) R. Lucio Porto, R. Frappier, J.B. Ducros, C. Aucher, H. Mosqueda, S. Chenu, B. Chavillon, F. Tessier, F. Cheviré, T. Brousse, *Electrochimica Acta*, **2012**, *82*, 257-262; (d) P. Simon, Y. Gogotsi, *Nature Mater*, **2008**, *7*, 845-854

[3] (a) S. Dong, X. Chen, L. Gu, X. Zhou, H. Xu, H. Wang, Z. Liu, P. Han, J. Yao, L. Wang, G. Cui, and L. Chen, *ACS Appl. Mater. Interfaces*, **2011**, *3*, 93–98 ; (b) Y.-S. Jun, W. H. Hong, M. Antonietti and A. Thomas, *Adv. Mater.* **2009**, *21*, 4270–4274

[4] (a) C. Giordano, C. Erpen, W. Yao, and M. Antonietti, *Nano Lett.*, **2008**, *8*, 4659-4663 ; (b) C. Giordano, C. Erpen, W. Yao, B. Milke, and M. Antonietti, *Chem. Mater.*, **2009**, *21*, 5136–5144; (c) C. Giordano, M. Antonietti, *Nano Today*, **2011**, *6*, 366—380

[5] (a) C. Boissiere, D. Grosso, A. Chaumonnot, L. Nicole, and C. Sanchez, *Adv. Mater.*, **2011**, *23*, 599–623 ; (b) G. L. Messing, S.-C. Zhang, and G. V. Jayanthi, *J. Am. Ceram. Soc*, **1993**, *76*, 2707-26

[6] (a) M. Kakati, B. Bora, S. Sarma, B.J. Saikia, T. Shripathi, U. Deshpand, Aditi Dubey, G. Ghosh, and A. K. Das, *Vacuum*, **2008**, *82*, 833–841 ; (b) E. A. Pruss, G. L. Wood, W. J. Kroenke, and R. T. Paine, *Chem. Mater.*, **2000**, *12*, 19-21 ; (c) Y. Takao, K. Shuzenji, and T. Tachibana, *J. Am. Ceram. Soc.*, **2008**, *91*, 311–314

[7] (a) M. Drygas, C. Czosnek, R. T. Paine, and J. F. Janik, *Chem. Mater.*, **2006**, *18*, 3122-3129; (b) M. Drygas, C. Czosnek, R. T. Paine, and J. F. Janik, *Mat. Res. Bull.*, **2005**, *40*, 1136–1142

[8] J. H. Bang, K. S. Suslick, *Adv. Mater.*, **2009**, *21*, 1–5

[9] Z. Jiang, W. E. Rhine, *Chem. Mater.*, **1991**, *3*, 1132-1137

[10] P. M. Schaber, J. Colson, S. Higgins, D. Thielen, B. Anspach, and J. Brauer, *Thermochim. Acta*, **2004**, *424*, 131–142

[11] (a) S. E. Rodil, *Diam. Relat. Mater.*, **2005**, *14*, 1262–1269 ; (b) P. Hammer, R.G. Lacerda, R. Droppa Jr., and F. Alvarez, *Diam. Relat. Mater.*, **2000**, *9*, 577–581

[12] N. Hering, K. Schreiber, and R. Riedel, O. Lichtenberger and J. Woltersdorf, *Appl. Organometal. Chem.*, **2001**, *15*, 879–886

[13] P. K. Chu, L. Li, *Mater. Chem. Phys.*, **2006**, *96*, 253–277

Entry for the Table of Contents

FULL PAPER

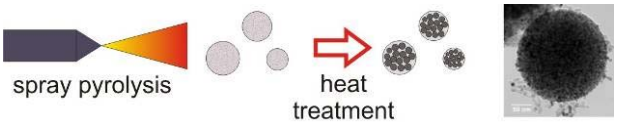

V. Maurice, G. Clavel, M. Antonietti, C. Giordano

Page No. – Page No.

Aerosol Assisted Synthesis of Porous TiN_xO_y@C Nanocomposites

Porous TiN_xO_y@C nanocomposites were prepared at relatively moderate temperature without the assistance of any template by coupling an aerosol process with the urea glass route. The relative specific surface area (up to 187 m^2/g) and porosity can be adjusted by changing reaction conditions.